IEEE Access
Multidisciplinary ⁝ Rapid Review ⁝ Open Access Journal

Received 17 June 2022, accepted 23 July 2022, date of publication 27 July 2022, date of current version 8 August 2022.
Digital Object Identifier 10.1109/ACCESS.2022.3194146

RESEARCH ARTICLE

Dynamic Waypoint Navigation: Model-Based Adaptive Trajectory Planner for Human-Symbiotic Mobile Robots

MITSUHIRO KAMEZAKI[1], (Member, IEEE), AYANO KOBAYASHI[2], RYOSUKE KONO[2], MICHIAKI HIRAYAMA[2], AND SHIGEKI SUGANO[2], (Fellow, IEEE)
[1]Waseda Research Institute for Science and Engineering, Waseda University, Shinjuku-ku, Tokyo 162-0044, Japan
[2]Department of Modern Mechanical Engineering, Waseda University, Shinjuku-ku, Tokyo 169-8555, Japan

Corresponding author: Mitsuhiro Kamezaki (kame-mitsu@aoni.waseda.jp)

This work was supported in part by the Japan Science and Technology Agency (JST) PRESTO under Grant JPMJPR1754; in part by the Japan Society for the Promotion of Science (JSPS) KAKENHI under Grant 19H01130; and in part by the Research Institute Science and Engineering, Waseda University.

This work involved human subjects or animals in its research. Approval of all ethical and experimental procedures and protocols was granted by the Ethics Review Committee of Waseda University under Application No. 2017-157.

ABSTRACT Path planning in dynamic environments is still a challenging issue with autonomous mobile robots. Current methods lack adaptability to various passing scenarios, a variety of passing trajectories including an acceleration path, or immediacy in planning time, which require human-aware navigation. In this study, we propose Dynamic Waypoint Navigation (DWN), which is a model-based adaptive real-time trajectory planning method. DWN first predicts human-robot path interference and the time and position of the interference on the basis of the measured velocity of humans. It then dynamically designates several waypoints considering the time delay of both calculation time and robot travel time. Then, DWN generates several trajectories by combining different speeds (default, acceleration, and deceleration) and paths (default, right, and left) and selects the best trajectory in terms of an interference-avoidance energy cost based on the degree of velocity-vector change. DWN can also output a trajectory within 0.5 s to immediately adapt to changes in human behavior and adopt a simple mathematical model and algorithm to enable easy expansion. Simulation and experimental results reveal that the DWN can adequately select a time-efficient trajectory in real-time and adaptively change a trajectory depending on human movement.

INDEX TERMS Autonomous mobile robot, dynamic waypoint navigation, path planning, real-time adaptive trajectory planning.

I. INTRODUCTION

Autonomous mobile robots that co-exist with humans are indispensable for various services such as human guidance, goods delivery, and manufacturing support [1], [2]. To achieve this, safe and efficient path planning is key, but path planning in 'dynamic environments' is still a challenging issue. As is well known and reviewed in many papers [3], [4], there are several approaches of path-planning methods suited to the characteristics of applied domains [5]. At the dawning age, grid (graph)-based methods overlay a grid on configuration space and assume each configuration is identified with a grid point. A∗ is used to find a path from the start to goal but is only applicable in static environments [6]. Artificial potential fields are used to treat a robot's configuration as a point in a potential field that combines attraction to the goal and repulsion from obstacles [7]. This method can fail to find a path or find a non-optimal path and does not explicitly control a velocity in dynamic situations. Sampling-based methods represent the configuration space with a roadmap of sampled configurations. Rapidly-exploring random trees (RRTs) incrementally construct a tree from samples drawn randomly

The associate editor coordinating the review of this manuscript and approving it for publication was Giulio Reina.

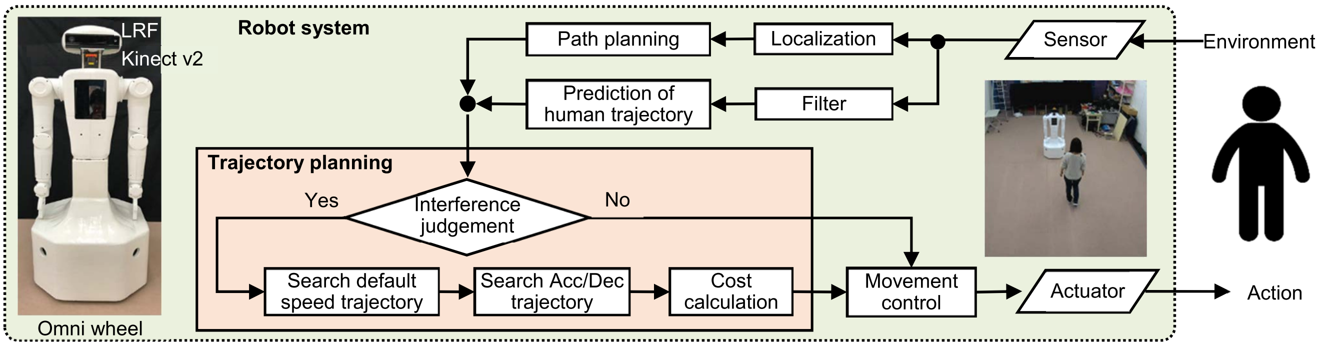

FIGURE 1. Relationship between integrated robot system and proposed trajectory-planning method. Sensors are a laser range finder (LRF) and RGB-D sensor (Kinect v2). Localization is made using a simple iterative closest point (ICP) algorithm. Velocity vector of human is estimated using a Kalman filter.

from the search space [8]. Several derivatives can handle moving obstacles, e.g., [9], but this method requires a long calculation time. The dynamic window approach (DWA) is an online collision avoidance method, which is derived from the dynamics of a robot and is designed to handle the constraints imposed by the limited velocities and accelerations of the robot [10]. Many derivatives can handle moving obstacles, e.g., [11], but those studies do not focus on directly planning a robot trajectory and experimental situations are simple. Path-planning methods for human avoidance have been developed, but some of them only change a moving direction, such as avoiding to the left or right without changing the velocity [12] or stopping or decelerating without changing the path [13]. Moreover, passing scenarios in those studies are limited to specific ones, such as only right angle [14] or facing angle. In the modern periods, more sophisticated algorithms in the field of dynamic path planning have been proposed, which include optimal reciprocal collision avoidance (ORCA)-based methods [15], self-adaptive harmony search algorithm [16], model-predictive control-based methods [17], social-force-based methods for crowd navigation [18], and deep reinforcement learning-based methods [19]. In particular, learning-based methods that a robot acquires an adequate navigation policy to adapt to dynamic and complex crowd environments are attractive approaches, but their computational cost and domain adaptation to the real world should be further investigated.

As referred above, there are an enormous number of navigation methods, and they are becoming more complex. At the same time, we can find room for improvement in terms of simplicity and adaptability. Thus, this study aims to provide a model-based adaptive path planning method as one option for dynamic trajectory planners for human-symbiotic mobile robots.

Robot navigation in human co-existence spaces requires the following functions. First, path-planning methods must handle dynamic obstacles, i.e., humans, and be able to predict a time and position when they may interfere with each other. In dynamic situations, the path-planning method must handle any passing angles and rapidly change the trajectory if needed. It also needs to find a path as a minimum-cost trajectory generated by combining an arbitrary path and speed, depending on the situation. For example, passing to the right while accelerating has a lower cost than detouring to the left while decelerating. This behavior may not only ensure its movement efficiency but also allow the humans to easily understand the robot's intent. The human-coexistence environment changes dynamically, so the robot needs a framework that can quickly execute a series of controls including environment recognition, trajectory planning, action execution, and re-planning and re-execution. Thus, we need a real-time adaptive trajectory planning method for human-symbiotic mobile robots. To achieve this, the path-planning method should have real-time adaptability, predict human movement, generate acceleration and deceleration paths, and work at any passing angles.

In this study, we focused on waypoint navigation methods, which are easy to implement and have expandability. They have been applied as global path planning methods to autonomous vehicles [20] and autonomous unmanned aerial vehicles [21]. Based on this, we newly developed a trajectory-planning method that includes a real-time waypoint setting algorithm that considers the relative velocities of robots and humans based on prediction, generation of multiple trajectory candidates with arbitrary velocity vectors, and cost-effective trajectory selection, suitable for real-time local trajectory planning. We call this new method 'Dynamic Waypoint Navigation (DWN).' We evaluated DWN through simulation and an real-robot experiment and confirmed that DWN is effective in planning trajectories in dynamic situations.

II. IMPORTANCE OF (MODEL-BASED) DWN

We consider a situation in which a human and robot are interfering with each other; when the robot changes its path, the human also avoids it in the same direction as the robot. As a reaction, conventional path-planning methods make the robot move to the left path, e.g., [12], but it would be more efficient to 'accelerate' and pass on the right path. The robot can execute more appropriate and efficient movements if the path-planning method can output an appropriate velocity vector depending on the situation. As stated above, current autonomous mobile robots do not 'intentionally' accelerate in a situation where the robot passes humans due to the conservative idea that the robot is inherently dangerous to humans and should unilaterally avoid them [22]. On the other hand, DWN can plan multiple trajectories with different speeds and paths.

The higher the complexity of the trajectory planning, the higher the computational cost [23]. When the robot moves in the real world and interacts with humans, the real-time property of trajectory planning is vital. Thus, DWN guarantees a time delay within an acceptable range. The real world constantly changes, so we cannot wait for the completion of the path planning of the robot. DWN can handle the time delay by a rapid control loop of (re-)execution and (re-)planning.

In sum, current methods lack adaptability to various passing scenarios, a variety of passing trajectories including an acceleration path, or immediacy in planning time, which require human-aware navigation. Thus, this study aims to develop a trajectory-planning method for generating arbitrary velocity vectors including assertive acceleration, to select a suitable trajectory depending on the situation and to execute real-time control so that the natural passing with a human can be achieved without impairing the real-time property. Another aim of this study is to seek a mode-based navigation method with high generality and adaptability (expandability), which would newly become one of the navigation-method options. To end this, we will make the mathematical model of the DWN, implement the model into the real robot, and evaluate the DWN by using the real environments.

III. DYNAMIC WAYPOINT NAVIGATION (DWN)

As Fig. 1 shows, with DWN, the possibility of interference between a robot and human is estimated from sensor data, and when this interference is estimated, a trajectory that avoids the human is planned. The DWN first generates default-speed avoidance trajectories on the left and right of the human (Fig. 2 (a)) then generates trajectories with acceleration and deceleration (Fig. 2 (b)). Finally, it selects the best (lowest-cost) trajectory for the robot from among the generated trajectories. Each function is explained with reference to Figs. 2 and 3.

A. INTERFERENCE JUDGEMENT

1) DEFINITION OF PERSONAL SPACE

Psychology indicates that humans have a psychological space called personal space (PS) where they feel psychological pressure and discomfort when that space is intruded upon. Humans usually move in a way that does not violate PS [24]. PS is variously defined by the distance, speed, direction of the body, density of people, and so on. In this study, we assumed an environment in which humans can be avoided without worrying about the surrounding humans. Based on this assumption, we defined the PS as a circle with a radius of L_{RP} and L_{HP}. Thus, the robot searches for trajectories that do not enter the PS critical distance L_{PS}, which is given by

$$L_{PS} = L_{RP} + L_{HP}. \tag{1}$$

In this study, we defined as $L_{RP} = 0.5$ m and $L_{HP} = 0.5$ m [25].

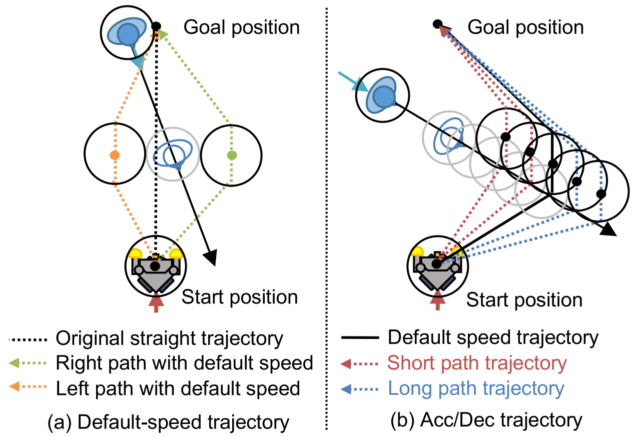

FIGURE 2. (a) Conceptual image of calculation flow to find trajectories. (b) Relative velocity vector determines if path needs acceleration or deceleration.

2) INTERFERENCE JUDGEMENT (FIG. 3 (A))

The positions of the robot and a human at the current time t_0 are $\vec{p}^{\,R}_{t_0} = [x^R_{t_0}, y^R_{t_0}]^T$ and $\vec{p}^{\,H}_{t_0} = [x^H_{t_0}, y^H_{t_0}]^T$. The robot position is estimated from a normal localization method and Kalman filter. The human position is estimated as the relative distance from the robot by using a laser range finder (LRF) [26]. The positions of the robot and human at an arbitrary time t are $\vec{p}^{\,R}_{t} = [x^R_{t}, y^R_{t}]^T$ and $\vec{p}^{\,H}_{t} = [x^H_{t}, y^H_{t}]^T$. Also, the difference between those times Δt is defined as $t - t_0$. The current speeds of the robot and human are $\vec{v}^{\,R}_{t_0} = [v^R_{xt_0}, v^R_{xt_0}]^T$ and $\vec{v}^{\,H}_{t_0} = [v^H_{xt_0}, v^H_{xt_0}]^T$. These positions at a time t can be also expressed as follows.

$$\vec{p}^{\,R}_{t} = \begin{bmatrix} x^R_t \\ y^R_t \end{bmatrix} = \begin{bmatrix} x^R_{t_0} \\ y^R_{t_0} \end{bmatrix} + \begin{bmatrix} v^R_{xt_0} \\ v^R_{yt_0} \end{bmatrix} \Delta t. \tag{2}$$

$$\vec{p}^{\,H}_{t} = \begin{bmatrix} x^H_t \\ y^H_t \end{bmatrix} = \begin{bmatrix} x^H_{t_0} \\ y^H_{t_0} \end{bmatrix} + \begin{bmatrix} v^H_{xt_0} \\ v^H_{yt_0} \end{bmatrix} \Delta t. \tag{3}$$

Next, the distance between the robot and human at t is calculated. We use a human-movement prediction model in which the human keeps a current velocity vector for simplification, but we can apply any prediction models, e.g., [27], [28]. First, the relative velocity vector $\vec{v}^{\,HR}_{t_0}$ (robot with respect to human) and relative position vector $\vec{p}^{\,HR}_{t_0}$ at t_0 are simply expressed as

$$\vec{v}^{\,HR}_{t_0} = \begin{bmatrix} v^{HR}_{xt_0} \\ v^{HR}_{yt_0} \end{bmatrix} = \begin{bmatrix} v^R_{xt_0} - v^H_{xt_0} \\ v^R_{yt_0} - v^H_{yt_0} \end{bmatrix}. \tag{4}$$

$$\vec{p}^{\,HR}_{t_0} = \begin{bmatrix} x^{HR}_{t_0} \\ y^{HR}_{t_0} \end{bmatrix} = \begin{bmatrix} x^R_{t_0} - x^H_{t_0} \\ y^R_{t_0} - y^H_{t_0} \end{bmatrix}. \tag{5}$$

Thus, the relative position vector $\vec{p}^{\,HR}_{t}$ at t is expressed as

$$\vec{p}^{\,HR}_{t} = \begin{bmatrix} x^{HR}_{t_0} \\ y^{HR}_{t_0} \end{bmatrix} + \begin{bmatrix} v^{HR}_{xt_0} \\ v^{HR}_{yt_0} \end{bmatrix} \Delta t. \tag{6}$$

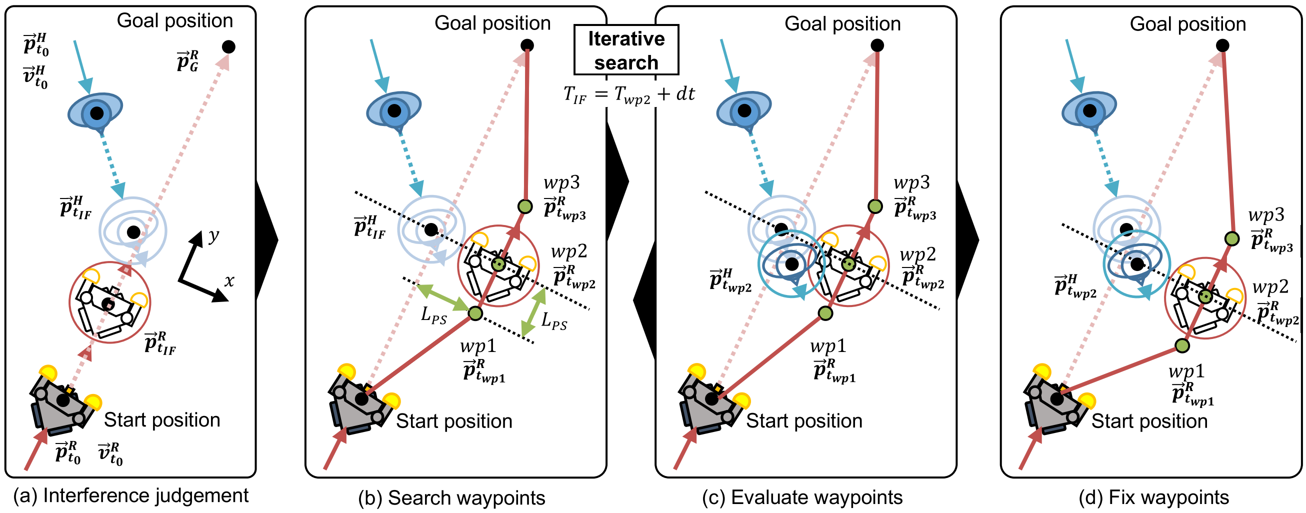

FIGURE 3. Calculation flow to find waypoints for default speed trajectory. (b) and (c): repeating search and correction to find waypoints where robot and human do not interfere with each other. This is an example of default-speed avoidance trajectory on right of human.

The square of the distance between the robot and human at t, $|\vec{p}_t^{HR}|^2$ is expressed as

$$|\vec{p}_t^{HR}|^2 = \left(x_{t0}^{HR} + v_{xt0}^{HR}\Delta t\right)^2 + \left(y_{t0}^{HR} + v_{xt0}^{HR}\Delta t\right)^2. \quad (7)$$

Organizing (7) for Δt gives (8).

$$a\Delta t^2 + b\Delta t + c = 0, \quad (8)$$

where, $a = v_{xt0}^{HR2} + v_{xt0}^{HR2}$ $b = 2\left(x_{t0}^{HR} v_{xt0}^{HR} + y_{t0}^{HR} v_{xt0}^{HR}\right)$ $c = x_{t0}^{HR2} + y_{t0}^{HR2} - |\vec{p}_t^{HR}|^2$. This means that no interference occurs when $\left|\vec{p}_t^{HR}\right| > L_{PS}$. On the other hand, interference occurs when $\left|\vec{p}_t^{HR}\right| \leq L_{PS}$. When interference occurs, Δt can be obtained from (8) and is defined as the interference time t_{IF}. The $\vec{p}_{t_{IF}}^R$ and $\vec{p}_{t_{IF}}^H$ obtained by substituting obtained t_{IF} into (2) and (3) are the respective interference positions.

B. GENERATION OF SET OF WAYPOINTS (WP)

1) TRAJECTORY WITH DEFAULT SPEED (FIGS. 3 (B)–(D))

On the basis of $\vec{p}_{t_{IF}}^H$ determined by the interference judgement, three waypoints (wp_1, wp_2, wp_3) for interference avoidance are defined, and each point is expressed as

$$\vec{p}_{t_{wp1}}^R = \left[x_{t_{wp1}}^R, y_{t_{wp1}}^R\right]^T$$
$$\vec{p}_{t_{wp2}}^R = \left[x_{t_{wp2}}^R, y_{t_{wp2}}^R\right]^T$$
$$\vec{p}_{t_{wp3}}^R = \left[x_{t_{wp3}}^R, y_{t_{wp3}}^R\right]^T. \quad (9)$$

We denote the difference between the robot's current position $\vec{p}_{t_0}^R$ and goal $\vec{p}_G^R = [x_G^R, y_G^R]^T$ as $\vec{p}_{CtoG}^R$, which is given by

$$\vec{p}_{CtoG}^R = \begin{bmatrix} x_G^R - x_{t0}^R \\ y_G^R - y_G^R \end{bmatrix}. \quad (10)$$

At this time, the coordinates of wp_1–wp_3 are obtained by (11)–(13), respectively. wp_2 is set at a point separated by L_{PS} just beside the human, and wp_1 and wp_3 are placed on the line passing wp_2 that is parallel to the moving direction of the robot. This setting can guarantee human avoidance.

$$\vec{p}_{t_{wp1}}^R = \vec{p}_{t_{wp2}}^R - L_{PS}\frac{\vec{p}_{CtoG}^R}{\left|\vec{p}_{CtoG}^R\right|} \quad (11)$$

$$\vec{p}_{t_{wp2}}^R = \vec{p}_{t_{IF}}^H + \begin{bmatrix} y_G^R - y_{t0}^R \\ x_{t0}^R - x_G^R \end{bmatrix} \cdot \frac{L_{PS}}{\left|\vec{p}_{CtoG}^R\right|} \quad (12)$$

$$\vec{p}_{t_{wp3}}^R = \vec{p}_{t_{wp2}}^R + L_{RP}\frac{\vec{p}_{CtoG}^R}{\left|\vec{p}_{CtoG}^R\right|} \quad (13)$$

The time t_{wp2} when the robot reaches wp_2 is given by

$$\left|\vec{p}_{t_{wp1}}^R - \vec{p}_{t_0}^R\right| + L_{PS} = \vec{v}_{t_0}^R(t_{wp2} - t_0) \quad (14)$$

At t_{wp2}, the human has already moved from $\vec{p}_{t_{IF}}^H$; thus, the robot and human will interfere with each other again, as shown in Fig. 3 (c). Thus, we set $t_{IF} = t_{wp2}$, and the robot searches for wp_2 so that the robot does not interfere with humans ($t_{IF} = t_{wp2}$) while shifting wp_2 repeatedly.

2) TRAJECTORY WITH ACCELERATION AND DECELERATION (FIG. 4)

The acceleration and deceleration trajectories are calculated by shifting wp_i and the speed required to reach wp_i with the distance d. As Fig. 4 shows, the robot shifts $\vec{p}_{t_{wp2}}^H$ at the passing time in the direction of velocity $\vec{v}_{t_0}^H$. When the shift is $\alpha \times d$, where $\alpha \in Z, \neq 0$, we denote the shifted point as $\vec{p}_{t_{wp2(\alpha d)}}^H$. Thus, $\vec{p}_{t_{wp2(\alpha d)}}^H$ and $\vec{p}_{t_{wp2(\alpha d)}}^R$ are obtained by (15) and (16), respectively. At this time, wp_1 and wp_3 can be

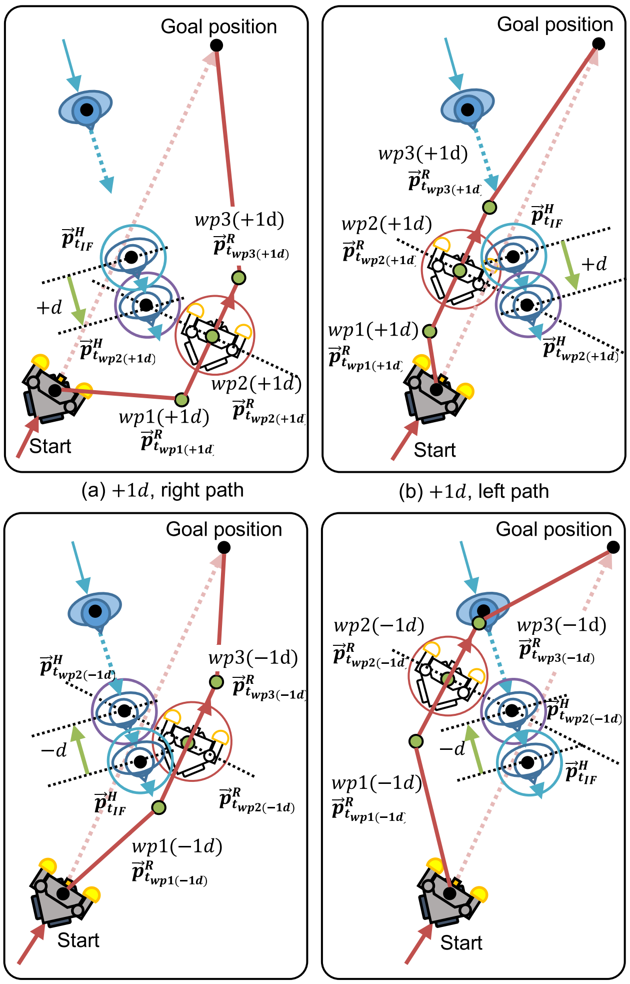

(a) $+1d$, right path (b) $+1d$, left path (c) $-1d$, right path (d) $-1d$, left path

FIGURE 4. Calculation flow to find waypoints for acceleration/deceleration trajectories. They are examples of shift distance = $+1d$ and $-1d$.

obtained from (17) and (18), respectively.

$$\vec{p}^H_{t_{wp2(\alpha d)}} = \vec{p}^H_{t_{wp2}} \pm \frac{\vec{v}^H_{t_0}}{\left|\vec{v}^H_{t_0}\right|} d \tag{15}$$

$$\vec{p}^R_{t_{wp2(\alpha d)}} = \vec{p}^H_{t_{wp2(\alpha d)}} + \begin{bmatrix} y^R_G - y^R_{t_0} \\ x^R_{t_0} - x^R_G \end{bmatrix} \cdot \frac{L_{PS}}{\left|\vec{p}^R_{CtoG}\right|} \tag{16}$$

$$\vec{p}^R_{t_{wp1(\alpha d)}} = \vec{p}^R_{t_{wp2(\alpha d)}} - L_{PS} \frac{\vec{p}^R_{CtoG}}{\left|\vec{p}^R_{CtoG}\right|} \tag{17}$$

$$\vec{p}^R_{t_{wp3(\alpha d)}} = \vec{p}^R_{t_{wp2(\alpha d)}} + L_{PS} \frac{\vec{p}^R_{CtoG}}{\left|\vec{p}^R_{CtoG}\right|} \tag{18}$$

Next, the passing times $t_{wp2(\alpha d)}$ and $t_{wp1(\alpha d)}$ for the robot to reach $wp1(\alpha d)$ are calculated, and the velocity $\vec{v}^R_{t_{wp1(\alpha d)}}$ required for the robot to finally pass through is determined.

$$t_{wp2(\alpha d)} = \frac{\vec{p}^H_{t_{wp2(\alpha d)}} - \vec{p}^H_{t_0}}{\left|\vec{v}^H_{t_0}\right|} \tag{19}$$

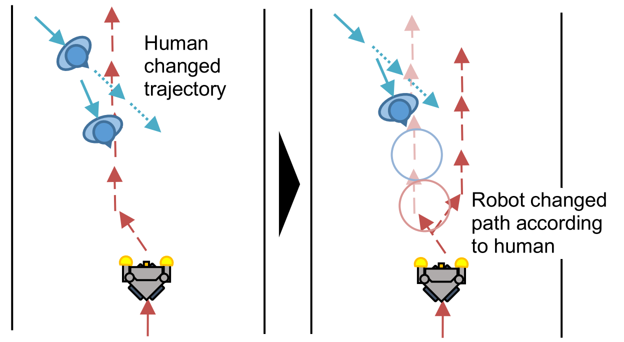

FIGURE 5. Trajectory re-planning according to change of human behavior.

$$t_{wp1(\alpha d)} = t_{wp2(\alpha d)} - \frac{\vec{p}^R_{t_{wp2(\alpha d)}} - \vec{p}^R_{t_{wp1(\alpha d)}}}{\left|\vec{v}^R_{t_0}\right|} \tag{20}$$

$$\vec{v}^R_{t_{wp1(\alpha d)}} = \frac{\vec{p}^R_{t_{wp1(\alpha d)}} - \vec{p}^R_{t_0}}{t_{wp1(\alpha d)} - t_0} \tag{21}$$

From the viewpoint of safety and security, when the robot passes at the closest approach to the human, that is, between wp_1 and wp_3, it passes at a default speed. The robot thus accelerates or decelerates from the current location to wp_1. Basically, after wp_2, the robot aims for the goal, and if the robot needs to return to the original path, we can set an additional waypoint wp_4 on the original trajectory. The robot iteratively executes the above calculation under the constraints of its limited motion (e.g., dynamics and size) and environments (e.g., walls and obstacles) [29]. We derive a total of eight types of trajectories, e.g., (a) right path-default speed, (b) left path-default speed, (c) default (straight) path with acceleration, (d) default (straight) path with deceleration, (e) right path acceleration, (f) right path with deceleration, (g) left path with acceleration, and (h) left path with deceleration.

As shown in Fig. 5, when the human suddenly changed his or her trajectory, the robot rapidly re-checks the interference. If they are interfering with each other, the robot re-plans the trajectory and quickly avoids the human.

C. DECISION OF TRAJECTORY BY COST CALCULATION

In this study, the behavior of the robot keeping a straight path at a constant speed was regarded as the lowest-cost (best) behavior. The acceleration or deceleration in the moving direction increases the cost. In addition, the larger the avoidance, the higher the cost. Thus, the movement of the robot in the lateral direction is also used as the cost-increasing parameter [30]. We denote $\vec{v}_{Gt}$ and $\vec{v}_{Gt_0}$ as a velocity vector in the movement direction of the robot at t and t_0 (default speed), respectively, $\vec{v}_{Dt}$ and $\vec{v}_{Dt-1}$ as a velocity vector in the direction of avoidance of the robot at t and $t-1$ (the time interval is 50 ms), respectively. The notation E_G is the energy in the movement direction, E_L is the energy in the direction of avoidance, and A and B are the weighting factors. We define the summation of the integration of the velocity difference from the start to goal in each direction as the trajectory

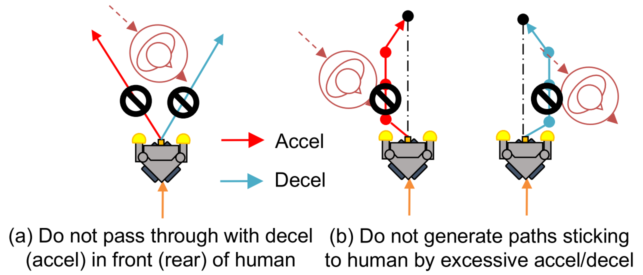

FIGURE 6. Reduction of calculation by heuristics.

cost E_T, and it is given by

$$E_T = E_G + E_L = A \int_{Start}^{End} \left| \vec{v}_{Gt}^2 - \vec{v}_{Gt0}^2 \right| dt + B \int_{Start}^{End} \left| \vec{v}_{Dt}^2 - \vec{v}_{Dt-1}^2 \right| dt \quad (22)$$

In the study, we set $A = B = 1$ (not weightened).

D. REAL-TIME ROBOT CONTROL

We need to consider sensing preciseness, calculation latency, and uncertainty of human behavior. DWN repeatedly generates several trajectories, so if the search range and search resolution are not set appropriately, the amount of calculation becomes enormous. We thus set the upper limit time for a robot-behavior generation to 0.5 s, according to a previous study [26], and reduced calculation time by applying the following heuristics.

- We assume that d shown in (15) is a minimum value that a human can recognize the difference in the robot trajectory, and set it to 10 cm (Fig. 2 (b)).
- Trajectories where the robot decelerates (accelerates) and passes in the front (rear) of the human (Fig. 6 (a)) and trajectories where the robot sticks to the human by excessive acceleration or deceleration (Fig. 6 (b)) obviously increase the cost, so the robot omits these trajectories.

As a result of applying these heuristics, the total calculation time required for the trajectory plan could be kept within 0.5 s. In addition, interference judgment as monitoring of environmental change was carried out at 1-s of intervals. DWN can cope with a reduction in computational complexity and quick re-planning. In addition to the above process, we consider the time delay of calculation beforehand (0.5 s). Specifically, we shift the time to 0.5 s in advance and generate trajectories. We also implement a controller that can take into account the dynamics of the robot. The robot smoothly connects each waypoint by using a spline curved interpolation method so as not to overshoot the planned trajectory.

IV. EXPERIMENTS

Again, the purpose of this study is to investigate the feasibility of DWN through simulation and real-robot experiments, not to compare other existing methods, since DWN's features are already explained in the previous sections. This study was approved by Ethics Review Committee on Research with Human Subjects of Waseda University. Written informed consent was obtained from each participant.

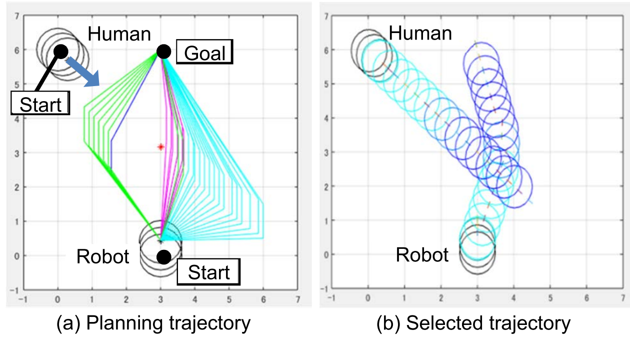

(c)

Type	Right	Left	Acc	Dec	R-Acc	L-Acc	R-Dec	L-Dec
Cost	0.50	1.39			0.28	0.61	0.54	

FIGURE 7. Simulation results from scenario 1.

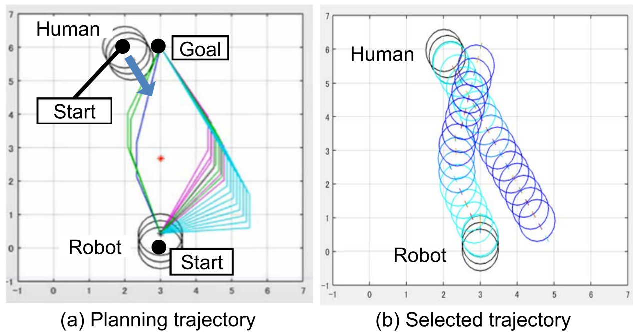

(c)

Type	Right	Left	Acc	Dec	R-Acc	L-Acc	R-Dec	L-Dec
Cost	2.22	0.37			1.33	1.26	2.22	2.22

FIGURE 8. Simulation results from scenario 2.

A. SIMULATION VALIDATION

1) SIMULATION CONDITIONS

We developed a simulator using MATLAB. We set an 8 × 8 m field with one robot and a human. The initial velocity of both the robot and human was 0.4 m/s or 0.7 m/s, and several patterns of the human initial position and moving directions were simulated. The passing scenarios included opposite, diagonal, and right-angle directions, and directional changes in the middle.

2) SIMULATION RESULTS

We present three examples of the simulation results. Figs. 7–9 illustrate (a) the planning trajectories including eight types of trajectories, (b) selected trajectory, and (c) cost value E_T of the trajectory candidates. The paths that were not generated due to kinematic and dynamic constraints have no values in the table. We found from Fig. 7 that DWN selected "right acceleration (0.28)" as the minimum cost. We also found that DWN selected "left (default speed) (0.37)" (Fig. 8) and that it selected "deceleration (default path) (0.68)" (Fig. 9).

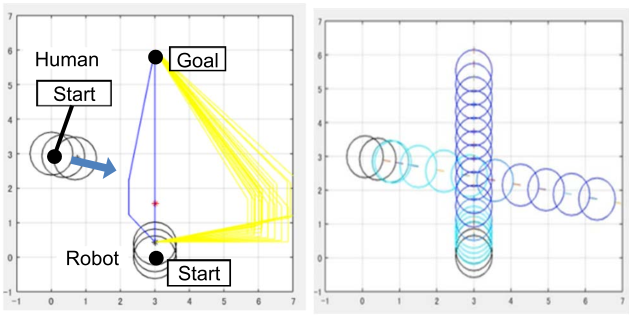

(a) Planning trajectory (b) Selected trajectory

(c)

Type	Right	Left	Acc	Dec	R-Acc	L-Acc	R-Dec	L-Dec
Cost		0.73		0.68				3.61

FIGURE 9. Simulation results from scenario 3.

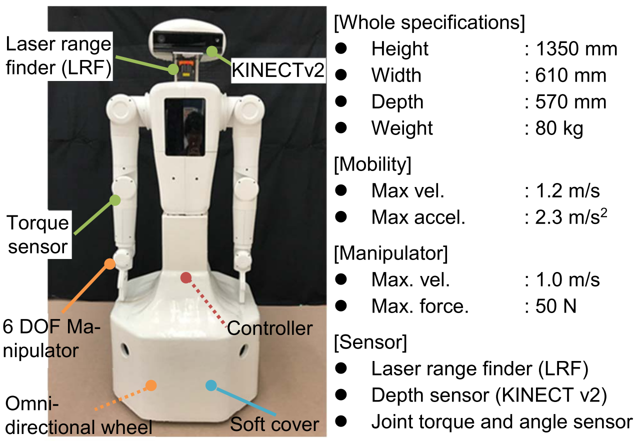

FIGURE 10. Specifications of mobile robot.

TABLE 1. Experimental conditions.

Item	Straight	Diagonal	Right	Change
Robot velocity (initial) m/s	0.4			
Human velocity (const.) m/s	0.4			
Distance to collision point m	3			
Passing angle deg	180	135	90	180→225

We confirmed that DWN could generate several trajectories and select the minimum cost trajectory with acceleration and deceleration depending on the situation.

B. REAL-ROBOT EXPERIMENT

1) EXPERIMENTAL CONDITIONS

We developed an autonomous mobile robot, as shown in Fig. 10. The robot has omnidirectional wheels and two 6-degrees-of-freedom (DOF) manipulators with torque and angle sensors. The robot also has an LRF and Kinect v2 (RGB-D sensor). We set a 10 × 10 m field with one robot and a human. The experimental conditions are listed in Table 1. We set the walking speed of humans as a constant 0.4 m/s. The initial velocity of the robot was 0.4 m/s, and four patterns of the human's initial position and moving directions were

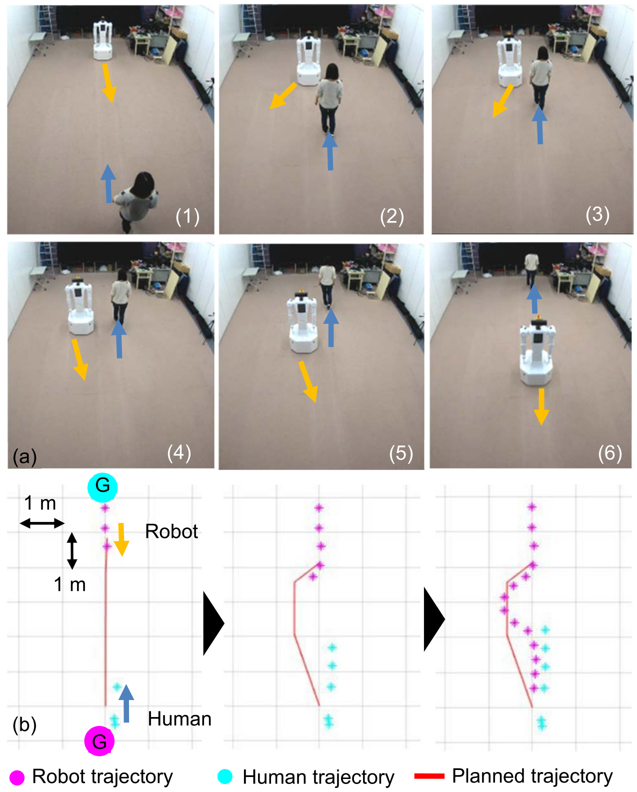

(c)

Type	Right	Left	Acc	Dec	R-Acc	L-Acc	R-Dec	L-Dec
Cost	0.80	1.79			0.69	1.67	0.74	1.60

FIGURE 11. Passing in straight opposite direction.

simulated, including straight opposite, diagonal, and right-angle directions, and changes in the middle. Human's initial positions were set to the ones so that the travel distance to a collision point for both the robot and human was around 3 m.

2) EXPERIMENTAL RESULTS

We present four examples of the experimental results. Figs. 11–14 indicate (a) scenes of passing situation, (b) planned trajectory of robot and actual trajectories of robot and human, (c) E_T of the trajectory candidate, for passing in the straight opposite direction (Fig. 11), passing in the diagonal opposite direction (Fig. 12), passing in the right-angle direction (Fig. 13), and change of human trajectory from the straight opposite direction to a diagonal direction (Fig. 14). The dots to indicate the actual trajectory were plotted every 1 second.

We found from Fig. 11 that DWN selected "right acceleration" which had a minimum cost of 0.69. The avoidance speed was accelerated from 0.4 to 0.43 m/s. We also found that DWN selected "right (default speed) (0.28)" (Fig. 12) and that it selected "right (default speed) (1.01)" (Fig. 13). In Fig. 13 (b), during a period just after starting walking, the velocity of humans continues to increase, so the robot re-planned the trajectory to avoid the human more laterally. We confirmed that DWN could generate several trajectories

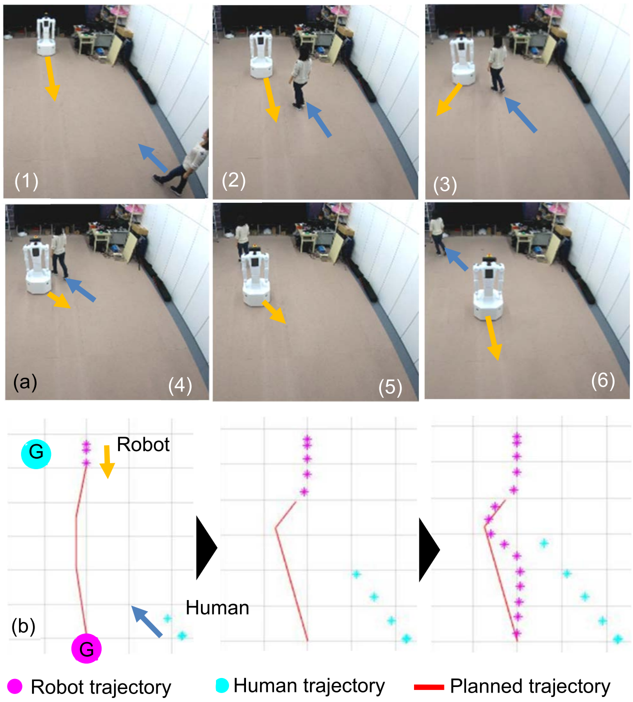

(c)

Type	Right	Left	Acc	Dec	R-Acc	L-Acc	R-Dec	L-Dec
Cost	0.28	2.13			0.29		0.29	

FIGURE 12. **Passing in diagonal opposite direction.**

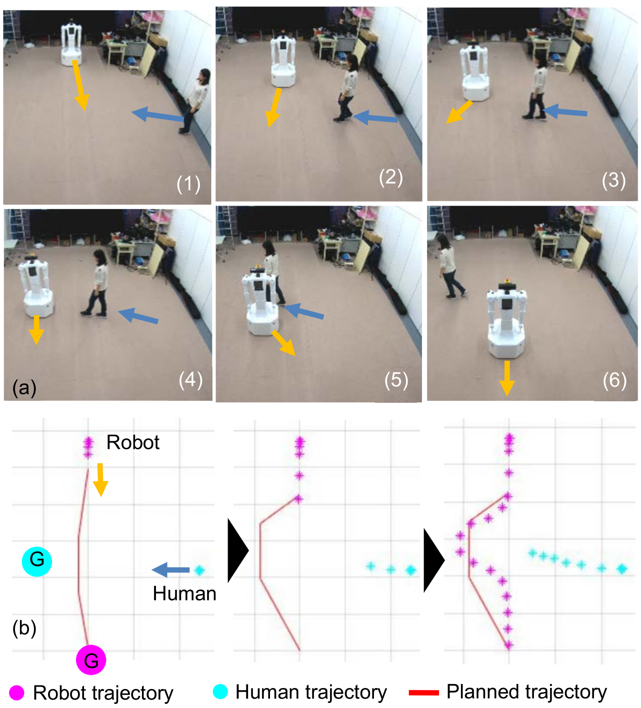

(c)

Type	Right	Left	Acc	Dec	R-Acc	L-Acc	R-Dec	L-Dec
Cost	1.01	1.98						

FIGURE 13. **Passing in right-angle direction.**

and select the minimum cost trajectory with acceleration and deceleration depending on the situation.

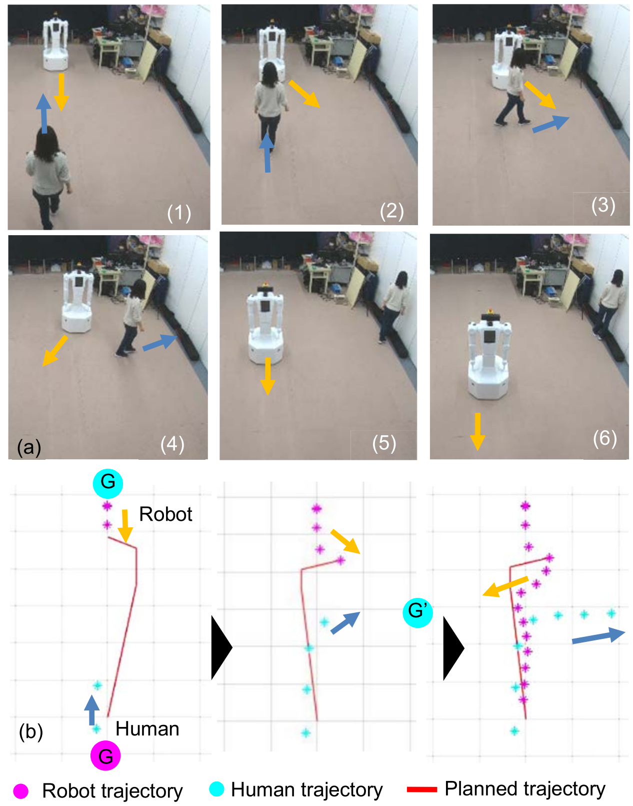

(c)

Type	Right	Left	Acc	Dec	R-Acc	L-Acc	R-Dec	L-Dec
Cost	1.48	0.11		3.12	1.32	0.18	1.60	0.30

↓

Type	Right	Left	Acc	Dec	R-Acc	L-Acc	R-Dec	L-Dec
Cost	0.86	1.09						

FIGURE 14. **Change of human trajectory from straight opposite direction to diagonal direction.**

We found from Fig. 14 that the DWN selected "left (default speed) (0.11)" and then "right (default speed) (0.86)." Figs. 14 (a-1) and (a-2) show that the robot recognized that the human was going straight from the opposite direction and first selected the trajectory for left avoidance and started to move to that trajectory. However, the robot immediately recognized that interference would occur since the human significantly changed her movement direction to the left (Fig. 14 (a-3)). As shown in Figs. 14 (a-4, 5, and 6), the robot selected the right avoidance trajectory in a short time and executed it to avoid the human without collision. We confirmed that the robot executed trajectory planning in real-time, and high response movement was possible. Specifically, all actual calculation times were less than 0.45 s at the distance of 6.0 m and less than 0.1 s at the distance of 1.0 m.

V. DISCUSSION

A. EXPANDABILITY TO ACTIVE INDUCEMENT STRATEGY

The passive avoidance strategy (PAS), where the robot finds a collision-free path, does not allow the robot to coordinate with humans. This will cause a freezing problem [30]. Thus, we previously proposed an active inducement strategy (AIS) to collaboratively move by conveying the intent of the robot to the human by using light signals, projection [32], gesture, voice, and physical touch [26], [33]. This AIS enables the robot to execute proximal navigation and provide more robust and efficient navigation in human-crowded spaces. We confirmed through experiments using an actual robot and humans that the AIS enabled the robot to move more efficiently and naturally by using inducement methods (e.g., path indication, voice interaction, and notifying touch) according to the situations (e.g., space attribute, available width, and the number of humans) [26]. DWN can easily generate an inducement trajectory so that the robot indicates its intent to pass near a human by setting waypoints that are shifted to the human side. We will make a DWN-based trajectory planning suited to AIS in the future.

B. FUTURE IMPROVEMENT

In this feasibility study, we demonstrated only the adaptive trajectory planning to avoid one person due to the limitation of the pages, but we have already confirmed the DWN's expandability to multiple-human avoidance in the simulation. Specifically, the robot continuously executes path planning one by one by considering avoiding chattering behaviors among humans and a deadlock state and reducing the calculation cost. The details of the mathematical model and implementation in a real robot will be reported in the future paper. We will apply more advanced methodologies in localization, human velocity-vector estimation, as well as real-time calculation algorithm, and construct a human-aware navigation system with DWN as a core.

VI. CONCLUSION AND FUTURE WORKS

In this study, we newly proposed Dynamic Waypoint Navigation (DWN) for human-symbiotic mobile robots. Specifically, DWN predicts human-robot path interference, and the time and position of the interference then dynamically designated several waypoints considering the time delay of both calculation time and robot travel time. DWN generates several trajectories by combining different speeds (default, acceleration, and deceleration) and paths (default, right, and left) and selects the best trajectory in terms of an interference-avoidance energy cost. In the simulation, we confirmed that the robot could select the trajectory with the minimum cost from several trajectory candidates, and in the real-robot experiment, we confirmed that DWN could generate trajectories in real-time, could select the lowest-cost behavior, and re-plan and re-execute. For the field of robot navigation, DWN would contribute to providing a new option that has a model-based simple but adaptive and expandable algorithm. DWN could be useful in industrial applications where are difficult to adopt data-driven approaches, e.g., deep learning, and need to combine other planning modules, such as monitoring, visual tracking, and precise manipulation.

In the future, we will plan to extend DWN to cope with scenarios in which multiple dynamic obstacles, e.g., humans in a station, exist and/or they move faster. Moreover, we further investigate by introducing DWN into other mobile platforms such as electric wheelchairs.

ACKNOWLEDGMENT

The authors would like to thank the Waseda Research Institute for Science and Engineering and the Future Robotics Organization of Waseda University.

REFERENCES

[1] T. Kruse, A. K. Pandey, R. Alami, and A. Kirsch, "Human-aware robot navigation: A survey," *Robot. Auto. Syst.*, vol. 61, no. 12, pp. 1726–1743, Dec. 2013.
[2] K. Dautenhahn, "Socially intelligent robots: Dimensions of human–robot interaction," *Phil. Trans. Roy. Soc. B, Biol. Sci.*, vol. 362, no. 1480, pp. 679–704, Apr. 2007.
[3] D. González, J. Pérez, V. Milanés, and F. Nashashibi, "A review of motion planning techniques for automated vehicles," *IEEE Trans. Intell. Transp. Syst.*, vol. 17, no. 4, pp. 1135–1145, Apr. 2016.
[4] A. Koubaa, H. Bennaceur, I. Chaari, S. Trigui, A. Ammar, M.-F. Sriti, M. Alajlan, O. Cheikhrouhou, and Y. Javed, "Introduction to mobile robot path planning," in *Robot Path Planning and Cooperation* (Studies in Computational Intelligence), vol. 772. Cham, Switzerland: Springer, 2018.
[5] M. Faisal, M. Algabri, B. M. Abdelkader, H. Dhahri, and M. M. Al Rahhal, "Human expertise in mobile robot navigation," *IEEE Access*, vol. 6, pp. 1694–1705, 2018.
[6] F. Duchoň, A. Babinec, M. Kajan, P. Beňo, M. Florek, T. Fico, and L. Jurišica, "Path planning with modified a star algorithm for a mobile robot," *Proc. Eng.*, vol. 96, pp. 59–69, Jan. 2014.
[7] Q. Yao, Z. Zheng, L. Qi, H. Yuan, X. Guo, M. Zhao, Z. Liu, and T. Yang, "Path planning method with improved artificial potential field—A reinforcement learning perspective," *IEEE Access*, vol. 8, pp. 135513–135523, 2020.
[8] A. Bry and N. Roy, "Rapidly-exploring random belief trees for motion planning under uncertainty," in *Proc. IEEE Int. Conf. Robot. Automat.*, May 2011, pp. 723–730.
[9] H. Yang, J. Lim, and S. Yoon, "Anytime RRBT for handling uncertainty and dynamic objects," in *Proc. IEEE/RSJ Int. Conf. Intell. Rob. Syst.*, Oct. 2016, pp. 4786–4793.
[10] O. Brock and O. Khatib, "High-speed navigation using the global dynamic window approach," in *Proc. IEEE Int. Conf. Robot. Automat.*, May 1999, pp. 341–346.
[11] D. H. Lee, S. S. Lee, C. K. Ahn, P. Shi, and C.-C. Lim, "Finite distribution estimation-based dynamic window approach to reliable obstacle avoidance of mobile robot," *IEEE Trans. Ind. Electron.*, vol. 68, no. 10, pp. 9998–10006, Oct. 2020.
[12] Y. Hosoda, K. Yamamoto, R. Ichinose, S. Egawa, J. Tamamoto, K. Tsubouchi, and S. Yuta, "Collision-avoidance algorithm for human-symbiotic robot," in *Proc. ICCAS*, Oct. 2010, pp. 557–561.
[13] S. Hamasaki, Y. Tamura, A. Yamashita, and H. Asama, "Prediction of human's movement for collision avoidance of mobile robot," in *Proc. IEEE Int. Conf. Robot. Biomimetics*, Dec. 2011, pp. 1633–1638.
[14] M. Kollmitz, K. Hsiao, J. Gaa, and W. Burgard, "Time dependent planning on a layered social cost map for human-aware robot navigation," in *Proc. Eur. Conf. Mobile Robots (ECMR)*, Sep. 2015, pp. 1–6.
[15] K. Guo, D. Wang, T. Fan, and J. Pan, "VR-ORCA: Variable responsibility optimal reciprocal collision avoidance," *IEEE Robot. Autom. Lett.*, vol. 6, no. 3, pp. 4520–4527, Jul. 2021.
[16] Y. Quan, H. Ouyang, C. Zhang, S. Li, and L.-Q. Gao, "Mobile robot dynamic path planning based on self-adaptive harmony search algorithm and morphin algorithm," *IEEE Access*, vol. 9, pp. 102758–102769, 2021.
[17] Y. Chen, F. Zhao, and Y. Lou, "Interactive model predictive control for robot navigation in dense crowds," *IEEE Trans. Syst., Man, Cybern. Syst.*, vol. 52, no. 4, pp. 2289–2301, Apr. 2022.
[18] X.-T. Truong and T. D. Ngo, "Toward socially aware robot navigation in dynamic and crowded environments: A proactive social motion model," *IEEE Trans. Autom. Sci. Eng.*, vol. 14, no. 4, pp. 1743–1760, Oct. 2017.
[19] L. Sun, J. Zhai, and W. Qin, "Crowd navigation in an unknown and dynamic environment based on deep reinforcement learning," *IEEE Access*, vol. 7, pp. 109544–109554, 2019.

[20] N. Wang and H. Xu, "Dynamics-constrained global-local hybrid path planning of an autonomous surface vehicle," *IEEE Trans. Veh. Technol.*, vol. 69, no. 7, pp. 6928–6942, Jul. 2020.
[21] S. Shair, J. H. Chandler, V. J. Gonzalez-Villela, R. M. Parkin, and M. R. Jackson, "The use of aerial images and GPS for mobile robot waypoint navigation," *IEEE/ASME Trans. Mechatron.*, vol. 13, no. 6, pp. 692–699, Dec. 2008.
[22] S. S. Samsani and M. S. Muhammad, "Socially compliant robot navigation in crowded environment by human behavior resemblance using deep reinforcement learning," *IEEE Robot. Autom. Lett.*, vol. 6, no. 3, pp. 5223–5230, Jul. 2021.
[23] H. Cheon and B. K. Kim, "Online bidirectional trajectory planning for mobile robots in state-time space," *IEEE Trans. Ind. Electron.*, vol. 66, no. 6, pp. 4555–4565, Jun. 2019.
[24] W. H. Warren and S. Whang, "Visual guidance of walking through apertures: Body-scaled information for affordances," *J. Experim. Psychol., Hum. Perception Perform.*, vol. 13, no. 3, pp. 371–383, 1987.
[25] E. T. Hall, "The hidden dimension," *Leonardo*, vol. 6, no. 1, p. 94, 1973.
[26] M. Kamezaki, A. Kobayashi, Y. Yokoyama, H. Yanagawa, M. Shrestha, and S. Sugano, "A preliminary study of interactive navigation framework with situation-adaptive multimodal inducement: Pass-by scenario," *Int. J. Social Robot.*, vol. 12, no. 2, pp. 567–588, May 2019.
[27] S.-Y. Chung and H.-P. Huang, "A mobile robot that understands pedestrian spatial behaviors," in *Proc. IEEE/RSJ Int. Conf. Intell. Robots Syst.*, Oct. 2010, pp. 5861–5866.
[28] Y. Tamura, P. D. Le, K. Hitomi, N. P. Chandrasiri, T. Bando, A. Yamashita, and H. Asama, "Development of pedestrian behavior model taking account of intention," in *Proc. IEEE/RSJ Int. Conf. Intell. Robots Syst.*, Oct. 2012, pp. 382–387.
[29] W. Yuan, Z. Li, and C.-Y. Su, "Multisensor-based navigation and control of a mobile service robot," *IEEE Trans. Syst., Man, Cybern. Syst.*, vol. 51, no. 4, pp. 2624–2634, Apr. 2021.
[30] C. Dondrup, C. Lichtenthäler, and M. Hanheide, "Hesitation signals in human-robot head-on encounters," in *Proc. ACM/IEEE Int. Conf. Human-robot Interact.*, Mar. 2014, pp. 154–155.
[31] C.-C. Yu and C.-C. Wang, "Collision- and freezing-free navigation in dynamic environments using learning to search," in *Proc. Conf. Technol. Appl. Artif. Intell.*, Nov. 2012, pp. 151–156.
[32] M. C. Shrestha, T. Onishi, A. Kobayashi, M. Kamezaki, and S. Sugano, "Communicating directional intent in robot navigation using projection indicators," in *Proc. 27th IEEE Int. Symp. Robot Human Interact. Commun. (RO-MAN)*, Aug. 2018, pp. 746–751.
[33] M. C. Shrestha, Y. Nohisa, A. Schmitz, S. Hayakawa, E. Uno, Y. Yokoyama, H. Yanagawa, K. Or, and S. Sugano, "Using contact-based inducement for efficient navigation in a congested environment," in *Proc. 24th IEEE Int. Symp. Robot Human Interact. Commun. (RO-MAN)*, Aug. 2015, pp. 456–461.

MITSUHIRO KAMEZAKI (Member, IEEE) received the B.S., M.S., and Dr.Eng. degrees in mechanical engineering from Waseda University, Tokyo, Japan, in 2005, 2007, and 2010, respectively. From 2007 to 2008, he was a Visiting Research Associate at the 21st Century COE Program, Waseda University. From 2008 to 2010, he was a Research Associate with the Global COE Program, Waseda University. From 2010 to 2013, he was a Research Associate with the Department of Modern Mechanical Engineering, Waseda University, where he is currently an Associate Professor with the Research Institute for Science and Engineering. His current research interests include intelligent machine systems, man–machine interface, and operator support system in operated-work machines. He is a member of IEEE RAS, SICE, RSJ, and JSME. He has received the Best Paper Award from the 11th Symposium on Construction Robotics in Japan, in 2008, the IROS Best Paper Award Finalist from the IEEE/RSJ IROS 2011, the SICE Young Author's Award Finalist from the 2013 SICE Annual Conference, the Young Investigation Excellence Award from RSJ, in 2016, the Best Paper Award from the IEEE/ASME AIM 2016, and the IEEE Robotics and Automation Letters Best Paper Award, in 2022.

AYANO KOBAYASHI received the B.S. and M.S. degrees in modern mechanical engineering from Waseda University, Tokyo, Japan, in 2016 and 2018, respectively. Her research interests include human–robot psychological model, autonomous mobile robots, and interactive navigation.

RYOSUKE KONO received the B.S. and M.S. degrees in modern mechanical engineering from Waseda University, Tokyo, Japan, in 2017 and 2019, respectively. His research interests include error-tolerant navigation, human-movement estimation, and autonomous mobile robots.

MICHIAKI HIRAYAMA received the B.S. and M.S. degrees in modern mechanical engineering from Waseda University, Tokyo, Japan, in 2018 and 2021, respectively. His research interests include dynamic path planning and self-parameter tunable autonomous mobile robots.

SHIGEKI SUGANO (Fellow, IEEE) received the B.S., M.S., and Dr.Eng. degrees in mechanical engineering from Waseda University, Tokyo, Japan, in 1981, 1983, and 1989, respectively. Since 1986, he has been a Faculty Member with the Department of Mechanical Engineering, Waseda University, where he is currently a Professor. Since 2014, he has been working as the Dean of the School/Graduate School of Creative Science and Engineering, Waseda University. His research interests include human-symbiotic anthropomorphic robot design, dexterous and safe manipulator design, and human–robot communication. From 2001 to 2010, he has served as the President for the Japan Association for Automation Advancement. In 2017, he has served as the President for SICE. He is a fellow of four academic societies, including The Japan Society of Mechanical Engineers (JSME), The Society of Instrument and Control Engineers (SICE), and The Robotics Society of Japan (RSJ). He has served as the General Chair for the IEEE/ASME International Conference on Advanced Intelligent Mechatronics, in 2003, and the IEEE/RSJ International Conference on Intelligent Robots and Systems, in 2013. He was the General Co-Chair of the 2006 IEEE/RSJ International Conference on Intelligent Robots and Systems (IROS2006) and the Program Co-Chair of the 2009 IEEE International Conference on Robotics and Automation (ICRA2009). He has also served as the General Co-Chair for the 2012 IEEE International Conference on Robotics and Automation (ICRA2012) and the Program Chair for the 2012 IEEE/ASME International Conference on Advanced Intelligent Mechatronics (AIM2012).